J. Biochem. **138**, 613–620 (2005)
doi:10.1093/jb/mvi164

NMR Analysis of the Mg^{2+}-Binding Properties of Aequorin, a Ca^{2+}-Binding Photoprotein

Wakana Ohashi[1], Satoshi Inouye[2], Toshio Yamazaki[1] and Hiroshi Hirota[1,*]
[1]RIKEN Genomic Sciences Center, 1-7-22, Suehiro, Tsurumi, Yokohama 230-0045; and [2]Yokohama Research Center, Chisso Corporation, 5-1 Okawa, Kanazawa, Yokohama 236-8605

Received June 15, 2005; accepted August 22, 2005

Aequorin, which is a calcium-sensitive photoprotein and a member of the EF-hand superfamily, binds to Mg^{2+} under physiological conditions, which modulates its light emission. The Mg^{2+} binding site and its stabilizing influence were examined by NMR spectroscopy. The binding of Mg^{2+} to aequorin prevented the molecule from aggregating and stabilized it in the monomeric form. To determine the structural differences between Mg^{2+}-bound and free aequorin, we have performed backbone NMR assignments of aequorin in the Mg^{2+}-free state. Mg^{2+} binding induces conformational changes that are localized in the EF-hand loops. The chemical shift difference data indicated that there are two Mg^{2+}-binding sites, EF-hands I and III. The Mg^{2+} titration experiment revealed that EF-hand III binds to Mg^{2+} with higher affinity than EF-hand I, and that only EF-hand III seems to be occupied by Mg^{2+} under physiological conditions.

Key words: bioluminescence, EF-hand, magnesium, NMR, photoprotein.

Abbreviations: DLS, dynamic light-scattering; MW, calculated molecular weight; R_H, hydrodynamic radius.

The photoprotein aequorin, isolated from the jellyfish *Aequorea aequorea* (synonyms *A. victoria or A. forskalea*), emits blue light by an intramolecular reaction upon Ca^{2+} binding (*1–4*), and it has been used as a probe to monitor Ca^{2+} concentrations in living cells (*5*, *6*). Aequorin consists of apoaequorin (apoprotein) and 2-hydroperoxycoelenterazine, which is formed from coelenterazine and molecular oxygen (*7*, *8*). When mixed with Ca^{2+}, aequorin emits light (λ_{max} = ~465 nm), and decomposes into apoaequorin, coelenteramide and CO_2. Apoaequorin comprises 189 amino acid residues in a single polypeptide chain (*9*, *10*). Homology searches revealed that aequorin has three EF-hand motifs characteristic of Ca^{2+}-binding sites (Fig. 1), and thus it has been classified as a member of the EF-hand superfamily, which includes calmodulin and troponin C. The EF-hand motif comprises two helices that flank a loop of 12 contiguous residues (*11*, *12*). Recent crystal structure analysis revealed that aequorin has four helix-loop-helix structures for the EF-hand domains (I, II, III and IV), and that the second EF-hand (II) domain cannot bind Ca^{2+} (*8*) due to a lack of Ca^{2+}-binding amino acid residues (Fig. 1).

As previously reported, results obtained on luminometric titration of native aequorin (*13*) and recombinant aequorin (*14*) with Ca^{2+} led to the conclusion that the number of Ca^{2+} ions required for the luminescence of aequorin is two, not three, per aequorin molecule. On the other hand, the titration of Ca^{2+} with a Ca^{2+}-sensitive electrode indicated that aequorin could bind more than two, probably three, Ca^{2+} (*14*). The luminescence of aequorin is triggered by two Ca^{2+}, and the binding-affinity of the first Ca^{2+} to aequorin is about 20 times higher than that of the third Ca^{2+}, which may be unrelated to light emission. However, whether two Ca^{2+}-binding sites exist among the three EF-hands for luminescence remains unclear.

The metal specificities of aequorin have been investigated (*15*, *16*), and Ca^{2+} and Sr^{2+} are suitable ions for light emission. Although Mg^{2+} and Ca^{2+} have similar chemical properties, Mg^{2+} shows different effects on the luminescence of aequorin: it decreases the calcium-independent light emission (*17*, *18*), the Ca^{2+} sensitivity (*19–22*) and the rate of luminescence. The EF-hands have been classified into Ca^{2+}/Mg^{2+}-type and Ca^{2+}-specific type on the basis of their selectivity and affinity for Mg^{2+} and Ca^{2+} (*23*). The Ca^{2+}/Mg^{2+}-type EF-hand binds Ca^{2+} with high affinity and Mg^{2+} with moderate affinity.

We studied the effect of Mg^{2+} on the structure of aequorin. The dynamic light scattering method was used for assessment of the aggregation of molecules and the stability of the monomeric state. Recently, we reported the NMR assignment of Mg^{2+}-bound aequorin (*24*). By comparing the NMR signals of Mg^{2+}-free aequorin with those of Mg^{2+}-bound aequorin, the binding sites of Mg^{2+} in aequorin were identified and the difference in the Mg^{2+} binding affinity was investigated by means of the Mg^{2+} titration method.

MATERIALS AND METHODS

Materials—Tris(hydroxymethyl)aminomethane (Tris), 2-(*N*-morpholino)ethanesulfonic acid (MES), KCl, $FeCl_3$ and $MgCl_2$ were purchased from Nacalai Tesque Inc. (Kyoto, Japan). LeMaster's medium, $(NH_4)_2SO_4$, ethylenediamine-*N,N,N′,N′*-tetraacetic acid (disodium salt: EDTA·2Na), and dithiothreitol were obtained from Wako Pure Chemicals (Osaka, Japan), and $MgSO_4$ was from Junsei Chemical (Tokyo, Japan). $^{15}NH_4Cl$ was purchased from Shoko Co. (Tokyo, Japan), D-[*U*-^{13}C]glucose and DL-1,4-[*U*-^{2}H]dithiothreitol were obtained from Isotec Inc.

*To whom correspondence should be addressed. Tel: +81-45-503-9211, Fax: +81-45-503-9210, E-mail: hirota@gsc.riken.jp

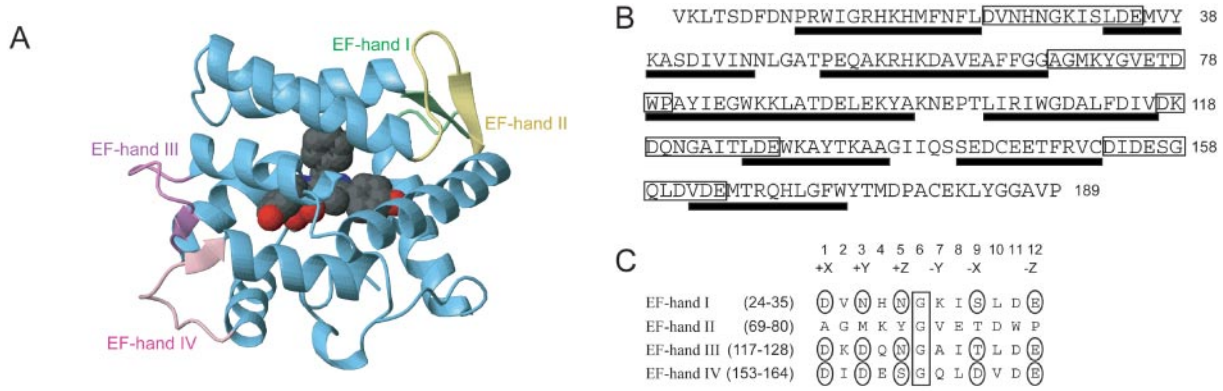

Fig. 1. **Ribbon representation, amino acid sequence and helix-loop-helix structure of the EF-hands in aequorin.** (A) Ribbon representation showing the secondary structure elements in the protein (PDB ID: 1EJ3). The loops of EF-hands are colored green (EF-hand I), yellow (EF-hand II), purple (EF-hand III), and pink (EF-hand IV). Coelenterazine is shown as a CPK representation. (B) The amino acid sequence of aequorin, and the helix regions of the EF-hands identified from the crystal structure study (*8*). The loops of EF-hands I-IV are shown in boxes and the helices of the EF-hand motifs are indicated with bars below the sequence. (C) The positions of each EF-hand loop are numbered 1–12, corresponding to amino acid residues 24–35 (EF-hand I), 69–80 (EF-hand II), 117–128 (EF-hand III), and 153–164 (EF-hand IV) in aequorin. The amino acid residues interacting with Ca^{2+} are circled, and ±X, ±Y, and ±Z are indicated as the coordinating positions in the pentagonal bipyramidal arrangement of Ca^{2+}. The –Y coordinating position is assumed to be the backbone carbonyl oxygen at the position of the 7th amino acid residue. The glycine residues conserved in the canonical EF-hand loops are boxed.

(Miamisburg, OH, USA), and [*U*-^{2}H]MES was from Cambridge Isotope Laboratories Inc. (Andover, MA, USA). All stable isotope enriched chemicals were >98 atom %.

Preparation of ^{15}N-Labeled and ^{13}C-, ^{15}N-Labeled Aequorin—Coelenterazine was chemically synthesized as previously reported (*25*). The recombinant aequorin used in this experiment consists of 191 amino acids, with an artificial modification at the N-terminus with the amino acid sequence of ANS instead of V in native aequorin (*9*, *26*, *27*). The procedures for the purification of recombinant aequorin were as follows (*28*). *E. coli* strain BL21 (Amersham Biosciences Corp., NJ, USA) was transformed with the expression vector piP-HE (*26*), and a single colony was grown in 10 ml of Luria-Bertani medium containing ampicillin (50 μg/ml) at 25°C for 15 h. The cultured cells were harvested by centrifugation at 5,000 × *g* for 5 min, suspended in 10 ml of M9-medium, and then added to 400 ml of M9-medium (^{13}C-glucose, 0.8 g; $^{15}NH_4Cl$, 0.4 g) and 0.01% Disfoam CE457 (a foam suppressant; NOF, Tokyo, Japan) in a 2 liter Erlenmeyer flask. After incubation at 37°C for 20 h on a rotary shaker (160 rpm/min), apoaequorin from the cells and the culture medium was used for aequorin preparation. To recover apoaequorin from the culture medium, the supernatant obtained by centrifugation at 5000 × *g* for 5 min was acidified with 1 M acetic acid to pH 4.6 and then the mixture was allowed to stand for 1 h at 4°C. A white precipitate formed and was collected by centrifugation at 12,000 × *g* for 10 min at 4°C. The precipitate containing apoaequorin was dissolved in 4 ml of 1 M Tris-HCl (pH 8.0). To obtain apoaequorin in cells, the cells were disrupted by sonication with a Branson model 200 sonifier in an ice bath. The suspension was centrifuged at 12,000 × *g* for 10 min at 4°C, and the pellet was discarded. Apoaequorin obtained from the culture medium and the cells was converted to aequorin and purified as previously described (*28*). The yield of ^{13}C-, ^{15}N-labeled aequorin was 10 mg from 400 ml of culture medium and cells.

Dynamic Light Scattering—Dynamic light scattering measurements were performed with a DynaPro molecular sizing instrument (DynaPro International Ltd., Milton Keynes, England) at 20°C, using a quartz scattering cuvette (12 μl). The instrument has a laser wavelength of 828.7 nm with a fixed scattering angle of 90°. The sample solutions, containing various concentrations of $(NH_4)_2SO_4$, KCl and $MgCl_2$ in 10 mM Tris-HCl (pH 7.0) with 3 mM EDTA, were passed through a filter (0.22 μm, Whatman) and then used for measurements. Averaged data were obtained for twenty points and were analyzed with Dynamics 6.3.40 software (DynaPro International Ltd.).

NMR Spectroscopy—All NMR spectra were measured at 20°C on Bruker AVANCE500, Bruker AVANCE600 and Bruker AVANCE800 spectrometers, equipped with pulsed field gradients and triple resonance probes. The resonance assignments for Mg^{2+}-bound aequorin were reported previously (*24*). The resonance assignments for the Mg^{2+}-free state of aequorin were obtained through HNCO, HNCA, HNCOCA, and ^{15}N NOESY-HSQC experiments with a 0.5 mM aequorin sample (uniformly labeled with ^{13}C and ^{15}N), in a buffer consisting of 10 mM Tris-d_{11} (pH 7.0), 3 mM EDTA, 100 mM KCl, and 10 mM dithiothreitol-d_{10} in 90% H_2O/10% D_2O. The samples used for the magnesium titration initially contained 0.2 mM 15N-labeled aequorin, in a buffer consisting of 10 mM MES-d_{13}, 0.1 mM EDTA, 100 mM KCl, and 10 mM dithiothreitol-d_{10} in 90% H_2O/10% D_2O, pH 6.6. Small aliquots of a 1 M $MgCl_2$ solution were added to the protein solution, and then two-dimensional ^{15}N HSQC spectra were recorded. The sample used for the Ca^{2+}-loaded aequorin contained 0.8 mM ^{15}N-labeled aequorin, in a buffer consisting of 20 mM MES-d_{13}, 100 mM KCl, 10 mM $CaCl_2$ and 10 mM dithiothreitol-d_{10} in 90% H_2O/10% D_2O, pH 6.6. All spectra were processed using NMRPipe (*29*), and were analyzed using NMRview (*30*) with a home built module, Kujira.

Table 1. **Effects of various salts on aequorin stability and aggregation. Calculated and measured values for the hydrodynamic radius (R_H) and the molecular weight (MW) of aequorin under various ionic conditions after 7 days.** Data with a monomodal distribution were analyzed using Dynamics 6.3.40 software.

No.	Salt	Salt concentration	0 days		7 days	
			R_H (nm)	MW (kDa)	R_H (nm)	MW (kDa)
1	$(NH_4)_2SO_4$	1.2 M	3.3	56	3.3	56
2	$(NH_4)_2SO_4$	10 mM	2.3	24	Multicomponents	
3	KCl	100 mM	2.5	28	Multicomponents	
4	KCl $MgCl_2$	100 mM 10 mM	2.3	21	2.3	22

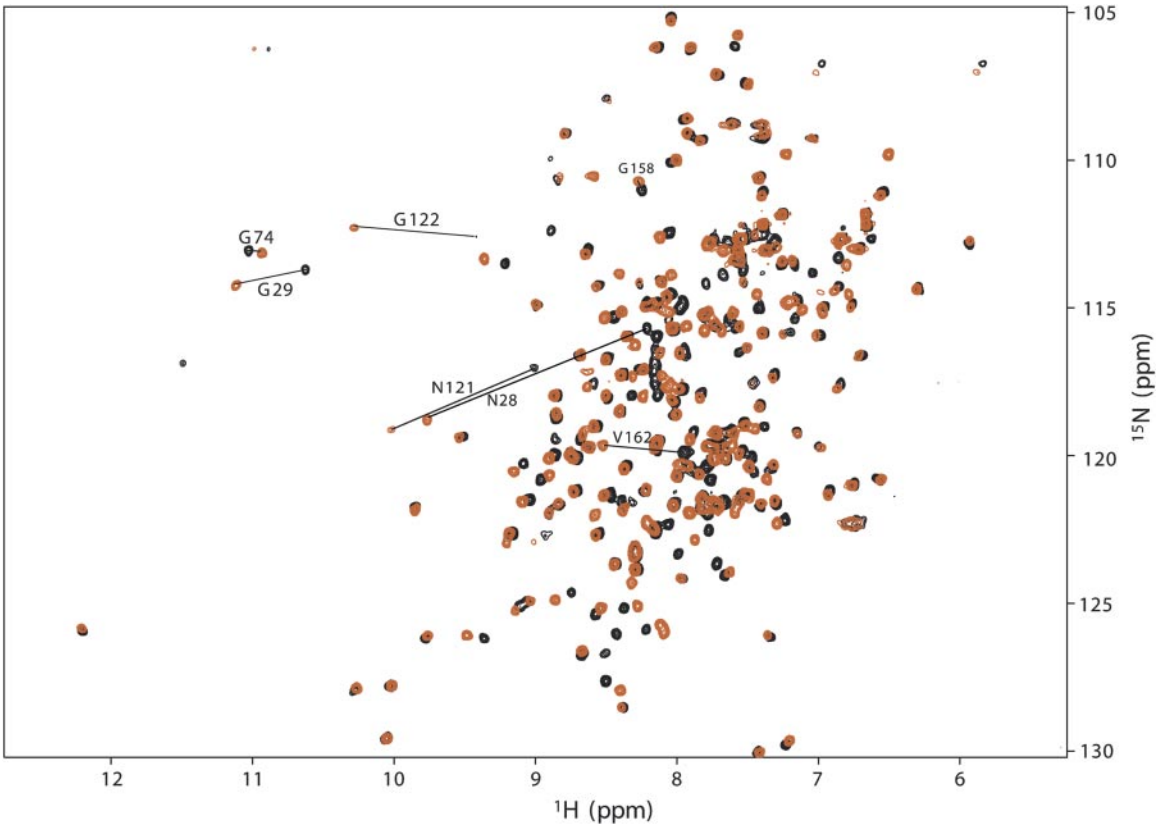

Fig. 2. **Superimposed ^1H-^{15}N HSQC spectra of ^{15}N-labeled aequorin in the presence and absence of Mg^{2+}.** The Mg^{2+} concentrations were 0 mM (red) and 10 mM (black), respectively. Labels indicate the glycines (G29, G74, G122, G158) located at position 6 of each EF-hand loop, N28 and N121 located at the +Z position of EF-hands I and III, respectively, and V162 located in the EF-hand IV loop.

RESULTS

Stability of Aequorin in Solution—In our preliminary studies involving heteronuclear ^1H-^{15}N correlation NMR (HSQC) analysis of ^{15}N-labeled aequorin at 20°C, aequorin dissolved in 10 mM MES buffer (pH 6.5) containing 100 mM KCl showed good dispersion. However, after 10 days, broad signals appeared in the middle region and signals exhibiting heterogeneous intensity were found in the ^1H-^{15}N HSQC spectra, suggesting that aequorin in solution formed aggregates and/or was denatured. For 2D and 3D NMR analyses, it is necessary to prevent protein aggregation and to stabilize the molecule. Dynamic light-scattering (DLS) analysis was employed to monitor the aggregation of aequorin in the presence of various salts.

The results of the DLS analysis under various conditions are summarized in Table 1. The effect of $(NH_4)_2SO_4$, which is known as a suitable stabilizer for aequorin, was examined. In the presence of 1.2 M $(NH_4)_2SO_4$, the molecular weight of 1 mM aequorin was estimated to be 56 kDa, indicating that aequorin was present in an oligomeric state. A lower concentration of $(NH_4)_2SO_4$ (10 mM) initially gave a monomer of 24 kDa, but the hydrodynamic radius and the calculated molecular mass increased after a week at 20°C, indicating that the protein became aggregated.

The addition of 100 mM KCl to a 1 mM aequorin solution in 10 mM Tris buffer (pH 7.0) containing 3 mM EDTA and 10 mM DTT initially generated a monodisperse size distribution around a molecular weight of 28 kDa, which is similar to that of the monomeric aequorin (Table 1, No. 3;

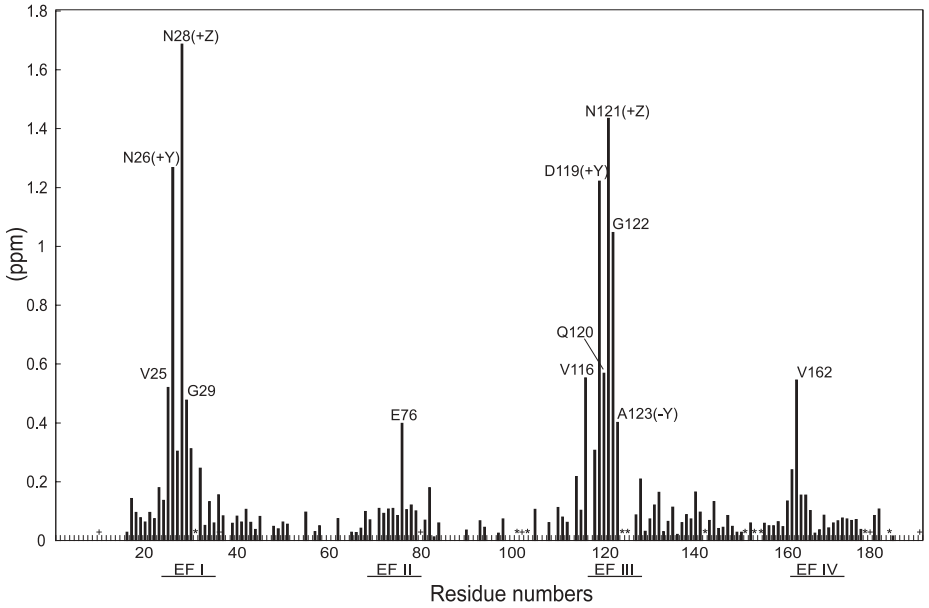

Fig. 3. **Absolute value differences of amide proton chemical shifts between Mg^{2+}-free and Mg^{2+}-bound aequorin.** The lines represent the average chemical shift differences. The loop regions of EF-hands I–IV are indicated by lines. Proline residues are indicated by plus (+) marks. The asterisks (*) represent uncalculated residues.

0 days). However, after a week at 20°C, a broad size distribution was observed and the molecular size had increased. These data revealed that the molecular state of aequorin was heterogeneous and that it became aggregated (Table 1, No. 3; 7 days), suggesting that KCl is not effective in preventing aequorin aggregation.

The addition of $MgCl_2$ to the above buffer improved the situation. After a week, the size distribution of aequorin observed on DLS analysis was narrow and monomodal, indicating the absence of aggregation. The hydrodynamic radius was 2.3 nm and the molecular weight estimated from the hydrodynamic radius was 22 kDa (Table 1, No. 4). This result clearly indicated that $MgCl_2$ has a profound stabilizing effect on monomeric aequorin.

Mg^{2+}-Bound and Free States—Since the Mg^{2+}-bound state of aequorin is more preferable for nuclear magnetic resonance (NMR) measurement than the Mg^{2+}-free state, we applied NMR spectroscopy to backbone assignment of the Mg^{2+}-bound state, as previously reported (*24*). To investigate the Mg^{2+} binding sites and the conformational changes induced by Mg^{2+}, backbone resonance assignment of the Mg^{2+}-free state of aequorin was performed. Due to the instability of the Mg^{2+}-free state, each sample solution of the Mg^{2+}-free aequorin was used within a week for the NMR measurements. Using the reported assignment results for the Mg^{2+}-bound state (*24*), the assignment of the Mg^{2+}-free state was performed using HNCA, HNCOCA, HNCO and ^{15}N NOESY-HSQC spectra. The slightly poor quality of the spectra of Mg^{2+}-free aequorin necessitated the use of a NOESY spectrum for the Mg^{2+}-free assignment. The ^{1}H-^{15}N HSQC spectra of aequorin at pH 6.6 are shown in Fig. 2, the Mg^{2+}-free aequorin exhibiting well-resolved peaks (Fig. 2, red). The HSQC spectra of the Mg^{2+}-bound and Mg^{2+}-free states of aequorin shared signal dispersion characteristics, suggesting that Mg^{2+} binding does not alter the global structure of aequorin. The glycine residues at G29, G74, G122 and G158 are located at the sixth position of the 12-residue loop in EF-hands I, II, III and IV, respectively. In a typical EF-hand motif, chemical shifts of the sixth glycine residue appear at low fields, as a consequence of the hydrogen bonding between the first amino acid residue and the sixth glycine residue of the EF-hand loop (*31–33*). The backbone assignments indicated that the ^{1}H signals of G29, G74 and G122 appeared in the low-field region, which are a typical feature of an EF-hand motif. On the other hand, G158 was observed in the middle region of the ^{1}H chemical shift, suggesting that the features of EF-hand IV differ from those of a typical EF-hand motif. The signals that appeared at different positions for the Mg^{2+}-bound and Mg^{2+}-free spectra were mainly assigned to the loop regions of EF-hands I, II, III and IV. The amide protons of residues I31 (loop I), D117 (loop III), I124 (loop III), T125 (loop III), L126 (loop III), D153 (loop IV), and I154 (loop IV) remain unassigned. The chemical shift difference values for the Mg^{2+}-bound and free states were plotted against the residue number (Fig. 3). Large chemical shift changes were observed for the Ca^{2+} binding loops of EF-hands I and III. In these EF-hand loops, N26, N28, D119, N121 and G122 exhibited large chemical shift changes. An EF-hand motif binds Mg^{2+} and Ca^{2+}, with the chelating loop residues at 1(+X), 3(+Y), 5(+Z), 7(–Y), 9(–X), and 12(–Z) arranged in an octahedral geometry with six oxygen atoms and a pentagonal bipyramidal geometry with seven oxygen atoms, respectively. In aequorin, N26 and D119 are located at the +Y position, and N28 and N121 at the +Z position in loops I and III, respectively. These data showed that Mg^{2+} can bind to EF-hands I and III, and that the amino acid residues positioned at +Y and +Z play an important role in Mg^{2+} binding. Although small chemical shift changes were observed in the loops of EF-hands II (E76) and IV (V162), other residues positioned at X, Y and Z that are involved in Ca^{2+} or Mg^{2+} coordination showed little or no chemical shift changes, indicating that Mg^{2+} did not bind to EF-hands II and IV. These data showed that Mg^{2+}-binding to EF-hands I and III did not change the global structure of aequorin, in spite of the alteration of the local conformation.

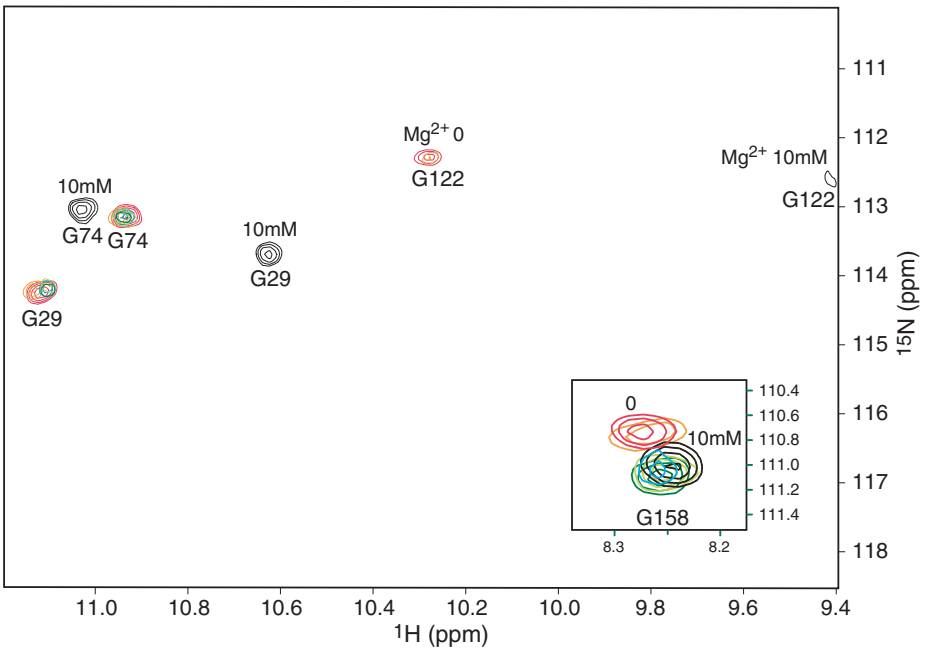

Fig. 4. **Selected regions of the ^{1}H-^{15}N HSQC spectra of aequorin, showing the G29, G74, G122 and G158 peaks with different concentrations of Mg^{2+}.** The inset shows the region of G158 located in the EF-hand IV loop. The glycine residues located at the 6 position of each EF-hand is numbered. The molar ratios of Mg^{2+} to aequorin are shown in colors: red, 0 (Mg^{2+}-free); yellow, 0.5 molar equiv.; cyan, 4 molar equiv.; pale green, 10 molar equiv.; green, 20 molar equiv.; black, 50 molar equiv. (10 mM). Peaks of G122 for 0.5, 4, 10 and 20 molar equiv. were not detected.

Mg^{2+} Titration—To obtain more detailed information on the effect of Mg^{2+} on aequorin, including the stoichiometry of Mg^{2+}, the site preference of Mg^{2+}-binding and the Mg^{2+}-induced conformational change, Mg^{2+} titration with uniformly ^{15}N-labeled aequorin was performed while 1H-^{15}N HSQC spectra were recorded. This technique, which monitors the backbone amide chemical shifts, is useful for investigating the protein structure and the global conformational changes. When Mg^{2+} was added to saturate EDTA in the aequorin solution, the intensities of the resonances corresponding to the EF-hand III and IV loops decreased, whereas the resonance intensities for the loops of EF-hands I and II remained unchanged (Fig. 4, yellow). When the concentration of Mg^{2+} reached 4 molar equivalents of aequorin (aequorin 0.2 mM, EDTA 0.1 mM and Mg^{2+} 0.9 mM; Fig. 4, blue), the resonance intensities for EF-hands I and II decreased and the signal positions did not change. On the other hand, the resonances corresponding to the loops of EF-hands III and IV, including G122 and G158, disappeared with substantial line broadenings and the signal positions shifted slightly. Such line broadening arises in the case when the rate of exchange between the Mg^{2+}-bound and Mg^{2+}-free states of aequorin is similar to the difference between the corresponding resonance frequencies. No further significant changes of the residues in EF-hands I and II were observed when 20 molar equivalents of Mg^{2+} were added to the sample (Fig. 4, pale green and green). In the presence of an excess amount of Mg^{2+} relative to the protein (aequorin 0.2 mM, EDTA 0.1 mM and Mg^{2+} 10 mM), the resonance frequencies of EF-hands I and II shifted, indicating that the affinity of EF-hand I is much lower than that of EF-hand III (Fig. 4, black). In the course of the titration, most of the resonances corresponding to the helical regions throughout the protein did not undergo appreciable chemical shift changes, suggesting that the conformational changes induced by Mg^{2+} binding were localized to only the loops of the EF-hands.

DISCUSSION

In this study, we have used NMR to identify the Mg^{2+} binding sites in aequorin and to determine the preference for Mg^{2+}. It is known that Mg^{2+} decreases the Ca^{2+}-dependent light emission of aequorin (*17*, *35*). Since the intracellular concentration of Mg^{2+} (10^{-3} M) is approximately 10^{2}–10^{4}-fold higher than that of Ca^{2+}, intracellular Mg^{2+} might have some effect on aequorin, in terms of the Ca^{2+}-triggered luminescent reaction in living cells.

Aequorin Stabilization on Mg^{2+} Binding—Our characterization of the Mg^{2+}-bound and metal-free states of aequorin has suggested that Mg^{2+} binding provides structural stability to the protein. The dynamic light scattering data clearly showed that Mg^{2+} stabilizes aequorin in the monomeric state for a week. Furthermore, the NMR and CD spectroscopic data demonstrated that the binding of Mg^{2+} to the EF-hand loops increases the structural stability of aequorin. In the metal-free state, temperature and time-dependent spectral changes were observed (data not shown). The CD spectrum of metal-free aequorin (10 μM) at 45°C shows a substantial reduction of the α-helix component, as compared to that obtained at 20°C. A smaller spectral change than that of the metal-free state is observed for aequorin with 0.3 mM Mg^{2+}. The contribution of Mg^{2+} to structural stability has also been observed with troponin C, and Mg^{2+} binding to the C-terminal EF-hands increases the structural stability (*36*, *37*). Similarly, the binding of Mg^{2+} to EF-hand III in aequorin may represent the most important contribution to the structural stability of aequorin.

EF-Hand II and IV, to Which Mg^{2+} Does Not Bind—Due to the lack of Ca^{2+}-binding amino acid residues, EF-hand II cannot bind to Ca^{2+}. The present NMR results show EF-hand II does not bind to Mg^{2+}. Although the chemical shift of the loop region of EF-hand II including E76 changed slightly, this is not due to the binding of Mg^{2+}. In the crys-

tal structure of the metal-free form of aequorin, the loop of EF-hand II is located close to the loop of EF-hand I, and a β-sheet structure is formed between E76–D78 of EF-hand II and K30–S32 of EF-hand I. Therefore, the structural change of EF-hand I loop that is induced by the binding of Mg^{2+} can lead to a slight change in the chemical shift of the EF-hand II loop including E76.

The NMR data showed that Mg^{2+} does not bind to EF-hand IV. This result was rather unexpected, since the loop of EF-hand IV is composed of canonical EF-hand sequences and possesses Ca^{2+} binding ability. The chemical shift of V162, located in the EF-hand IV loop, changed slightly, but this does not indicate Mg^{2+}-binding to this region. In the crystal structure of aequorin in the Ca^{2+}-free state, the amide proton of V162 forms a hydrogen bond with the carbonyl oxygen of G122, located in the loop of EF-hand III (*8*). It is reasonable to conclude that the resonance of V162 changes as a consequence of the rearrangement of the hydrogen bond network of Mg^{2+}-bound EF-hand III. In our study, a hydrogen bond between the residues at the first and sixth positions of the EF-hand IV loop was not detected, and the chemical shifts of V151, D153 and I154 located in the loop of EF-hand IV remained unassigned. In the crystal structure of the Ca^{2+}-free state of aequorin, the hydrogen bond network is disrupted and the loop structure in the loop of EF-hand IV is deformed, as compared to in other EF-hand loops (*8*, *38*). The NMR and X-ray data consistently show that the loop conformation of EF-hand IV differs from the canonical one and that it exhibits structural flexibility. This may be a reason why EF-hand IV is not suitable for Mg^{2+} binding. The affinities of EF-hands I, III and IV for Ca^{2+} have been investigated by using synthetic peptide fragments (20–22 amino acid residues) of the EF-hand loops, and the dissociation constants for Ca^{2+} showed the binding affinity order of III, I and IV (*39*). This order agrees well with that found in our Mg^{2+} binding experiments. These results imply that aequorin has the same binding preference for Ca^{2+} and Mg^{2+}.

Mg^{2+} Binding to Aequorin under Physiological Conditions—The Mg^{2+} titration experiments on aequorin involving NMR revealed that EF-hand III is a high Mg^{2+} affinity site and that EF-hand I is a low affinity site. This is the first report of the metal-binding preferences of the EF-hands in aequorin. Titration experiments showed that the Mg^{2+} affinities of EF-hand III and EF-hand I are 0.2–1 mM and 2–10 mM (K_{Mg}), respectively. Since no data were available regarding the direct interaction of Mg^{2+} with each of the binding sites in aequorin, these results provide a new insight into the interaction of Mg^{2+} with aequorin. As the intracellular concentration of Mg^{2+} is in the 10^{-3} M range, this level would only facilitate Mg^{2+} binding to EF-hand III. Therefore, our results suggest that in the absence of an intracellular Ca^{2+} stimulus, the predominant form of aequorin within the cell would be Mg_1-aequorin (Fig. 5). The affinity (K_D) of Ca^{2+} for aequorin was reported to be 13 μM (*34*), and that the affinity of Mg^{2+} for aequorin is much weaker than that of Ca^{2+}. When Ca^{2+} binds to aequorin in the presence of excess Mg^{2+}, such as under intracellular conditions, EF-hand III occupied by Mg^{2+} would interfere with Ca^{2+}-binding to this site, which would reduce the light emission. The presence of 1 mM Mg^{2+} decreases the Ca^{2+}-dependent luminescence (*21*).

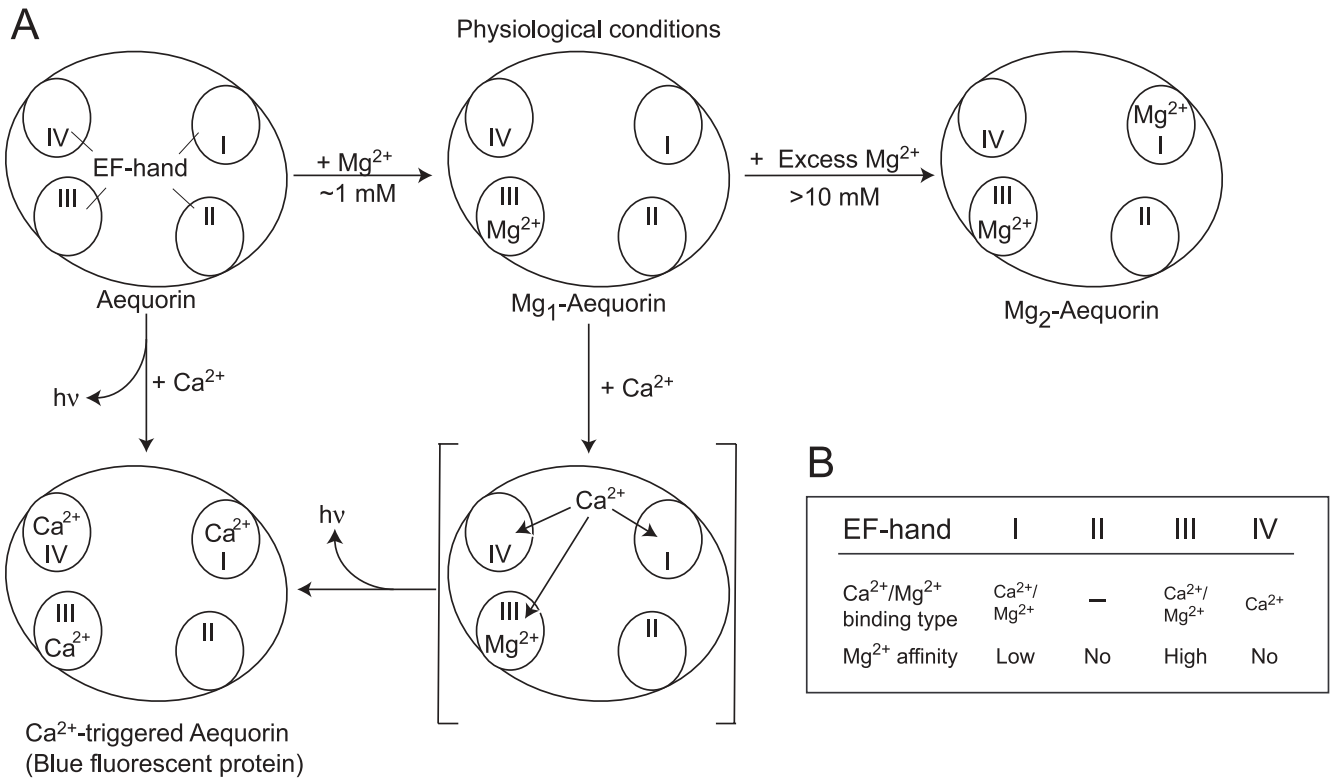

Fig. 5. **Model of Mg^{2+} and/or Ca^{2+} binding to aequorin.** (A) The aequorin binding equilibria with various concentrations of Mg^{2+} and Ca^{2+}. (B) The Mg^{2+}/Ca^{2+} binding types of EF-hands and the order of affinity for Mg^{2+} binding to aequorin.

Our results suggest that the inhibition is caused by the binding of Mg^{2+} to EF-hand III. Since EF-hand I exhibits low affinity for Mg^{2+} and is considered to exist in the free form with a physiological Mg^{2+} concentration, the Mg^{2+} effects on EF-hand I in terms of Ca^{2+}-binding and luminescence would probably be weaker than those on EF-hand III. The conformational change induced by Mg^{2+} is only localized in the loops of the EF-hands of aequorin, the other part remaining unchanged. Only the peaks assigned to the EF-hand loop regions exhibit different chemical shifts in the Mg^{2+}-bound and free HSQC spectra. A local conformational change induced by Mg^{2+} has also been observed for other EF-hand proteins. In both calmodulin and troponin C, the binding of Ca^{2+} to the EF-hand induces conformational changes including interhelical angle rearrangements (*32*, *33*), although the proteins also undergo local structural changes induced by Mg^{2+} (*40*, *41*). The ^{1}H-^{15}N HSQC spectrum of Ca^{2+}-bound aequorin showed good dispersion, suggesting that Ca^{2+}-bound aequorin is folded (data not shown). However, there are some different features from the Mg^{2+}-bound state: the number of signals increases, and the signal intensity becomes heterogeneous and distorted, indicating that Ca^{2+}-bound aequorin assumes several conformations. It is proposed that the binding of Ca^{2+} to aequorin induces large conformational changes, as observed for other EF-hand proteins.

In conclusion, our results demonstrate that aequorin has two Mg^{2+} binding sites located within the EF-hands. Among the three functional EF-hands (I, III and IV), only EF-hands I and III serve as Mg^{2+} binding sites. The affinity of EF-hand III for Mg^{2+} is stronger than that of EF-hand I. EF-hand III exhibits physiologically relevant affinity for Mg^{2+}. The Mg^{2+}-induced conformational change occurs locally within the EF-hand loops, the rest of the protein structure remaining unchanged. The binding of Mg^{2+} to the EF-hand stabilizes the aequorin molecule in the monomeric state. The stabilization by Mg^{2+} facilitated the collection of two-dimensional and three-dimensional NMR spectroscopic data, and the backbone assignment of the Mg^{2+}-bound state. The backbone assignment of the Mg^{2+}-bound state of aequorin provides information about the backbone assignment of the metal-free state and the Mg^{2+}-binding properties of aequorin.

This work was supported in part by the National Project on Protein Structural and Functional Analyses of the Ministry of Education, Culture, Sports, Science and Technology of Japan, and in part by the Program for Promotion of Fundamental Studies in Health Science of the Pharmaceutical and Medical Devices Agency (PMDA) of Japan (to S.I.).

REFERENCES

1. Shimomura, O., Johnson, F.H., and Saiga, Y. (1962) Extraction, purification and properties of aequorin, a bioluminescent protein from the luminous hydromedusan. *Aequorea*. *J. Cell. Comp. Physiol.* **59**, 223–240
2. Shimomura, O. and Johnson, F.H. (1979) Chemistry of the calcium-sensitive photoprotein aequorin. In *Detection and Measurement of Free Calcium Ions in Cells* (Ashley, C.C. and Campbell, A.K., eds.) pp. 73–83, Elsevier, North Amsterdam
3. Shimomura, O. (1983) Bioluminescence. *Photochem. Photobiol.* **38**, 773–779
4. Shimomura, O. and Johnson, F.H. (1976) Calcium-triggered luminescence of the photoprotein aequorin. *Symp. Soc. Exptl. Biol.* **30**, 41–54
5. Blinks, J.R., Prendergast, F.G., and Allen, D.G. (1976) Photoproteins as biological calcium indicators. *Pharmacol. Rev.* **28**, 1–93
6. Blinks, J.R. (1985) In *Bioluminescence and Chemiluminescence: Instrumental Applications* (K. Van Dyke, ed.) Vol. 2. pp. 185–226, CRC, Boca Raton, FL
7. Shimomura, O. and Johnson, F.H. (1978) Peroxidized coelenterazine, the active group in the photoprotein aequorin. *Proc. Natl. Acad. Sci. USA* **75**, 2611–2615
8. Head, J.F., Inouye, S., Teranishi, K., and Shimomura, O. (2000) The crystal structure of the photoprotein aequorin at 2.3 Å resolution. *Nature* **405**, 372–376
9. Inouye, S., Noguchi, M., Sakaki, Y., Takagi, Y., Miyata, T., Iwanaga, S. Miyata, T., and Tsuji, F.I. (1985) Cloning and sequence analysis of cDNA for the luminescent protein aequorin. *Proc. Natl. Acad. Sci. USA* **82**, 3154–3158
10. Charbonneau, H., Walsh, A.K., McCann, R.O., Prendergast, F.G., Cormier, M.J., and Vanaman, T.C. (1985) Amino acid sequence of the calcium-dependent photoprotein aequorin. *Biochemistry* **24**, 6762–6771
11. Kretsinger, R.H. and Nockolds, C.E. (1973) Carp muscle calcium-binding protein. II. Structure determination and general description. *J. Biol. Chem.* **248**, 3313–3326
12. Kawasaki, H., Nakayama, S., and Kretsinger, R.H. (1998) Classification and evolution of EF-hand proteins. *Biometals* **4**, 277–295
13. Shimomura, O. (1995) Luminescence of aequorin is triggered by the binding of two calcium ions. *Biochem. Biophys. Res. Commun.* **211**, 359–363
14. Shimomura, O. and Inouye, S. (1996) Titration of recombinant aequorin with calcium chloride. *Biochem. Biophys. Res. Commun.* **221**, 77–81
15. Izutsu, K.T., Felton, S.P., Siegel, I.A., Yoda, W.T., and Chen, A.C.N. (1972) Aequorin: its ionic specificity. *Biochem. Biophys. Res. Commun.* **49**, 1034–1039
16. Shimomura, O. and Johnson, F.H. (1973) Further data on the specificity of aequorin luminescence to calcium. *Biochem. Biophys. Res. Commun.* **53**, 490–494
17. Allen, D.G., Blinks, J.R., and Prendergast, F.G. (1977) Aequorin luminescence: relation of light emission to calcium concentration - a calcium-independent component. *Science* **196**, 996–998
18. Ray, B.C., Ho, S., Kemple, M.D., Prendergast, F.G., and Nageswara Rao, B.D.N. (1985) Proton NMR of aequorin. Structural changes concomitant with calcium-independent light emission. *Biochemistry* **24**, 4280–4287
19. Moisecu, D.G., Ashley, C.C., and Campbell, A.K. (1975) Comparative aspects of the calcium-sensitive photoproteins aequorin and obelin. *Biochim. Biophys. Acta* **369**, 133–140
20. Illarionov, B.A., Frank, L.A., Illarionova, V.A., Bondar, V. S, Vysotski, E.S., and Blinks, J.R. (2000) Recombinant obelin: Cloning and expression of cDNA, purification, and characterization as a calcium indicator. *Methods Enzymol.* **305**, 223–249
21. Moisescu, D.G. and Ashley, C.C. (1977) The effect of physiologically occurring cations upon aequorin light emission. Determination of the binding constants. *Biochim. Biophys. Acta* **460**, 189–205
22. Hastings, J.W., Mitchell, G., Mattingly, P.H., Blinks, J.R., and van Leeuwen, M. (1969) Response of aequorin bioluminescence to rapid changes in calcium concentration. *Nature* **222**, 1047–1050
23. Potter, J.F. and Gergely, J. (1975) The calcium and magnesium binding sites on troponin and their role in the regulation of

myofibrillar adenosine triphosphatase. *J. Biol. Chem.* **250**, 4628–4633
24. Ohashi, W., Inouye, S., Yamazaki, T., Doi-Katayama, Y., Yokoyama, S., and Hirota, H. (2005) Backbone ^{1}H, ^{13}C and 15N resonance assignments for the Mg^{2+}-bound form of the Ca^{2+}-binding photoprotein aequorin. *J. Biomol. NMR* **31**, 375–376
25. Inoue, S., Sugiura, S., Kakoi, H., Hasuzume, K., Goto, T., and Iio, H. (1975) Squid bioluminescence II. Isolation from *Watasenia scintillans* and synthesis of 2-(*p*-hydroxybenzyl)-6-(*p*-hydroxyphenyl)-3,7-dihydroimidazo[1,2-*a*]pyrazin-3-one. *Chem. Lett.* 141–144
26. Inouye, S., Aoyama, S., Miyata, T., Tsuji, F.I., and Sakaki, Y. (1989) Overexpression and purification of the recombinant Ca^{2+}-binding protein, apoaequorin. *J. Biochem.* **105**, 473–477
27. Inouye, S., Zenno, S., Sakaki, Y., and Tsuji, F.I. (1991) High-level expression and purification of apoaequorin. *Protein Expres. Purif.* **2**, 122–126
28. Shimomura, O. and Inouye, S. (1999) The *in situ* regeneration and extraction of recombinant aequorin from *Escherichia coli* cells and the purification of extracted aequorin. *Protein Expres. Purif.* **16**, 91–95
29. Delaglio, F., Grzesiek, S., Vuister, G.W., Zhu, G., Pfeifer, J., and Bax, A. (1995) NMRPipe: a multidimensional spectral processing system based on UNIX pipes. *J. Biomol. NMR* **6**, 277–293
30. Johnson, B. and Blevins, R. (1994) NMRView: a computer program for the visualization and analysis of NMR data. *J. Biomol. NMR* **4**, 603–614
31. Ikura, M., Minowa, O., Yazawa, M., Yagi, K., and Hikichi, K. (1987) Sequence-specific assignments of downfield-shifted amide proton resonances of calmodulin. *FEBS Lett.* **219**, 17–21
32. Spyracopoulos, L., Li, M.X., Sia, S.K., Gagne, S.M., Chandra, M., Solaro, R.J., and Sykes, B.D. (1997) Calcium-induced structural transition in the regulatory domain of human cardiac troponin C. *Biochemistry* **36**, 12138–12146
33. Zhang, M., Tanaka, T., and Ikura, M. (1995) Calcium-induced conformational transition revealed by the solution structure of apo calmodulin. *Nat. Struct. Biol.* **2**, 758–767
34. Kendall, J.M., Sala-Newby, G., Ghalaut, V., Dormer, R.L., and Campbell, A.K. (1992) Engineering the Ca^{2+}-activated photoprotein aequorin with reduced affinity for calcium. *Biochem. Biophys. Res. Commun.* **187**, 1091–1097
35. Allen, D.G. and Blinks, J.R. (1978) Calcium transients in aequorin-injected frog cardiac muscle. *Nature* **273**, 509–513
36. Szczesna, D., Guzman, G., Miller, T., Zhao, J., Farokhi, K., Ellemberger, H., and Potter, J.D. (1996) The role of the four Ca^{2+} binding sites of troponin C in the regulation of skeletal muscle contraction. *J. Biol. Chem.* **271**, 8381–8386
37. Zot, H.G. and Potter, J.D. (1982) A structural role for the Ca^{2+}-Mg^{2+} sites on troponin C in the regulation of muscle contraction. Preparation and properties of troponin C depleted myofibrils. *J. Biol. Chem.* **257**, 7678–7683
38. Toma, S., Chong, K, T., Nakagawa, A., Teranishi, K., Inouye, S., and Shimomura, O. (2005) The crystal structures of semi-synthetic aequorins. *Protein Sci.* **14**, 409–416
39. Oishi, O., Nagatomo, A., Kohzuma, T., Oda, N., Miyazima, T., Ohno, M., and Sakaki, Y. (1992) Validity of putative calcium binding loops of photoprotein aequorin. *FEBS Lett.* **307**, 272–274
40. Finley, N.L., Howarth, J.W., and Rosevear, P.R. (2004) Structure of the Mg^{2+}-loaded C-lobe of cardiac troponin C bound to the N-domain of cardiac troponin I: comparison with the Ca^{2+}-loaded structure. *Biochemistry* **43**, 11371–11379
41. Ohki, S., Ikura, M., and Zhang, M. (1997) Identification of Mg^{2+}-binding sites and the role of Mg^{2+} on target recognition by calmodulin. *Biochemistry* **36**, 4309–4316